Fracture failure representation of quasi-brittle materials using a three-dimensional dipole BEM formulation including loading rate effects

L.P.R. Almeida[1], Edson D. Leonel[1]

[1]*Dept. of Structural Engineering, São Carlos School of Engineering, University of São Paulo*
Av. Trabalhador São- Carlense, 400 – Parque Arnold Schimidt, 13566-590, São Carlos – SP, Brazil
luisphilipealmeida@usp.br, edleonel@sc.usp.br

Abstract. This study presents an alternative boundary element method (BEM) formulation for the cohesive crack propagation modelling in three-dimensional structures, including loading rates problems. Therefore, these developments enable the modelling of viscous-cohesive fracture processes. An initial stress field for representing the mechanical behaviour along the fracture process zone is proposed, which leads to a set of self equilibrated forces named as dipole. The proposed dipole-based formulation demonstrates some advantages in comparison to classical BEM approaches in this field. Among them, it is worth citing the discretisation of only one crack surface and the requirement of solely three integral equations per source point at the crack surface. Then, in addition to the accuracy, the proposed formulation is efficient in terms of computational effort, which is especially high in three-dimensional problems. Cohesive laws govern the material nonlinear behaviour along the fracture process zone. The mechanical effects of loading rate over the material resistance at the FPZ are properly handled by a time dependent function, which modifies the tensile material strength and the material fracture energy as a function of the loading velocity rate. Some applications are introduced to demonstrate the adequate performance of the proposed formulation, in which the results obtained have been compared against experimental responses available in the literature.

Keywords: Viscous-cohesive crack propagation; Dipole-based formulation; 3D BEM.

1 Introduction

The study and prediction of structural behaviour are essential in any engineering project, whether in civil construction, aeronautics or in the automotive field. In particular, the search for robust and efficient methodologies is stimulated by the need for increasing complex structures, in which both high mechanical performance and low weight are desired. In this context, research in structural engineering becomes essential, and is interested in developing suitable theories for predicting the mechanical behaviour of structures, identifying possible failure and collapse scenarios.

Nonlinear fracture of quasi-brittle materials has often been modelled by the cohesive fracture mechanics approach, in which cohesive stresses represent the residual strength of the material at the FPZ. Then, the fictitious crack replaces the FPZ and cohesive stresses close the fictitious crack surfaces. Furthermore, quasi-static conditions are often assumed in such modelling [1]. However, some experimental studies [2, 3] demonstrate that the loading rate largely modifies the material's resistance behaviour at the FPZ. The peak load increases monotonically with increasing loading rates, while the value of the displacement associated with the peak load remains practically the same [4]. According to Rush et al.[5], the mechanical response of concrete is directly influenced by the loading rate. Higher loading rates implies in higher initial stiffness, higher peak value stresses and higher slopes after the peak during rate-controlled tests. Then, the inclusion of loading rate effects is justified, aiming to find a model closer to the real behaviour of structures. These may be influenced by different loading rates, resulting from wind actions, movement of people, vehicle traffic, equipment action and/or explosions [6].

In this context, the mechanical failure of almost brittle materials can be represented through the association of a numerical method, such as BEM, and models derived from fracture mechanics, which enable the representation of the nonlinear dissipation effect in the fracture process zone (FPZ). This zone is small enough in comparison with the crack length in purely brittle materials, which leads to linear elastic fracture mechanics (MFEL). Therefore, at MFEL, the nonlinear effects can be disregarded. However, the FPZ is not small enough in quasi-brittle materials, which triggers nonlinear effects that must be accounted for for accurate mechanical modelling. Then, nonlinear fracture problems can be adequately addressed by an alternative formulation of the BEM based on an initial stress field, which represents the nonlinear material behaviour along the FPZ and leads to the concept of dipoles of stress. In this alternative approach, the domain term of the classical singular integral equation is degenerate and non-null only on the crack surfaces. As this term has its dimension reduced by one, a dipole associated with the initial stress field appears and govern the nonlinear behaviour of the material at the FPZ [7–10].

In this work, the dipole-based BEM formulation is extended to the 3D approach considering viscous-cohesive crack propagation problems. The three classical cohesive laws, Linear, Bilinear and Exponential, are updated in order to account the viscous effects. Further, the hypersingular kernels present in this formulation are regularized with the Guiggiani technique [11, 12] and an example is presented in order to show the robustness of the 3D viscous-cohesive dipole-based BEM formulation.

2 Dipole-based BEM integral formulation

The starting point for the proposed formulation is based on the classic BEM integral equation [13], which takes into account a domain Ω and a boundary Γ term. The domain term includes the presence of an initial stress term σ^0_{jk}, as suggested by [14], as follows:

$$c_{lk}u_k + \int_\Gamma p^*_{lk}u_k \, d\Gamma = \int_\Gamma u^*_{lk}p_k \, d\Gamma + \int_\Omega \sigma^0_{jk}\varepsilon^*_{ljk} \, d\Omega_0 \tag{1}$$

where Ω_0 represents the domain of non-zero values of σ^0_{jk}.

The last term of Equation 1 can be rewritten knowing that $p^l_j = \sigma^0_{jk}\eta_k$ represents the tractions at the narrow region of the boundary associated to the FPZ. Besides the solution of general cohesive crack growth problems requires the evaluation of such terms into the global coordinate system:

$$\int_{\Omega_0} \sigma^0_{jk}\varepsilon^*_{ljk} \, d\Omega_0 = \int_{\Gamma^c} 2a\frac{\partial u^*_{lj}}{\partial x_l}p^{0l}_j d\Gamma^c = \int_{\Gamma^c} 2a\frac{\partial u^*_{lj}}{\partial X_l}\overline{p}^{0l}_{jd}\Gamma^c \tag{2}$$

The cohesive problem can be solved using a numerical scheme, taking into account the definition of a narrow FPZ. However, in such a case, the nonlinear zone needs to be wide enough to guarantee finite values of the initial stress field. Then, a singular stress field appears along the FPZ when the thickness tends to zero, which can be adequately explained by the nature of the problem. Taking this into account, the thickness of the FPZ can be assumed to be null and the integral terms of Equation 2 can be evaluated by defining a new tensor for the problem. Such important variable is here called a dipole, q, and is mathematically described below:

$$q^l_j = 2a\overline{p}^{0l}_j \tag{3}$$

Dipoles are sets of self-balanced forces that are introduced with the goal of superimposing the stress state associated with external loading at the FPZ. This superposition of stresses corrects the mechanical behaviour based on a set of constitutive laws, as well as the cohesive laws used in this work. Thus, the nonlinear behaviour of the material can be adequately modelled by this approach. The dipoles are included in the BEM integral representation through a domain term, since such term represents the nonlinearities in the problem domain. In addition, this tensor introduces finite values, when $2a \Rightarrow 0$, the forces internal to FPZ tend to infinity. Thus, the set of dipoles are responsible for maintaining the physical meaning of the stresses at the FPZ.

In this way, based on the integral terms presented in Equation 2, the integral kernels are defined to represent the mechanical behaviour in the process zone, which are defined as follows:

$$\sigma^0_{jk}\varepsilon^*_{ljk} \, d\Omega_0 = \int_{\Gamma^c} 2a\frac{\partial u^*_{lj}}{\partial X_l}\overline{p}^{0l}_j d\Gamma^c = \int_{\Gamma^c} G^l_{lj}q^l_j\Gamma^c \tag{4}$$

where $G^l_{lj} = \frac{\partial u^*_{lj}}{\partial X_l}$

The components of the integral kernels of the tensor G^l_{lj} are presented in detail in Almeida et al. [7–10]. Its explicit representation is introduced below:

$$G^l_{ij} = \frac{1}{16\pi}(1-v)\mu r^2\{-(3-4v)r_{,l}\delta_{lj} + r_{,j}\delta_{li} + r_l\delta_{lj} - 3r_{,i}r_{,l}r_{,j}\} \tag{5}$$

where δ is the Kronecker delta and $r_{,i}$ are the derivatives of the distances between the source point and the field point.

Thus, Equation 1 can be rewritten in the following form, taking into account the previous algebraic manipulations presented:

$$c_{lk}u_k + \int_{\Gamma} p^{*}_{lk}u_k \, d\Gamma = \int_{\Gamma} u^{*}_{lk}p_k \, d\Gamma + \int_{\Gamma^c} G^{l}_{ij}q^{l}_{j}d\Gamma^{c} \tag{6}$$

This last equation enables the solution of the boundary value problem taking into account the effects of material nonlinearities at the FPZ.

3 Algebraic representation

The last section described the necessary mathematical manipulations to transform the domain integral term into BEM boundary integral equations for modelling stresses and displacements, accounting the initial stress field. These procedures led to additional terms G^{l}_{ij}, for displacement values, and G^{ml}_{ij}, for stress values, which are evaluated along the FPZ.

The algebraic representation of these integral kernels was obtained after approximating the geometry and mechanical fields, using interpolation functions, as usual via BEM. In this work, Lagrangian linear quadrilateral interpolation functions are introduced to approximate these parameters [10]. Thus, the discretization at the boundary leads to the well-known influence matrices H and G, which define the displacements and surface forces at the boundary [9]. The dipole terms associated with K, for displacement values, and KS, for dipoles values. Finally, Equation 6 assume the following algebraic representation:

$$HU = GP + KQ \tag{7}$$

$$\sigma + H^{'}U = G^{'}P + KSQ \tag{8}$$

Equation 8 is obtained with the derivatives of Equation 7 and applying into the hook law[9]. K and KS are matrices that contain the influence terms associated with the Q dipoles.

The solution to the non-linear problem requires the manipulation of Equation 7 and Equation 8. Initially, the boundary conditions are introduced in Equation 7. As usual in the classic BEM formulation, the vector X stores the unknown boundary values while the vector F contains the prescribed boundary values:

$$AX = BF + KQ \Rightarrow \tag{9}$$

where the classic procedure of changing columns between the matrices H and G takes the matrices A and B. Matrix B stores the influence terms associated with the prescribed values at the boundary, while the matrix A contains the influence terms related to the unknown values in the contour. The parameters M and R are defined as follows: $M = A^{-1}BF$ and $R = A^{-1}K$. The introduced boundary conditions modify Equation 8, as follows:

$$\sigma + A^{'}X = B^{'}F + KSQ \Rightarrow \sigma = N + SQ \tag{10}$$

the parameters $A^{'}$ and $B^{'}$ appear after the process of changing columns between the matrices $H^{'}$ and $G^{'}$. The variables N and S are defined below: $N = B^{'}F - A^{'}M$ and $S = KS - A^{'}R$

The algebraic representations, Equation 9 and Equation 10, must be evaluated numerically by introducing the Gauss-Legendre quadrature. Furthermore, the regularisation scheme for hyper singular kernels proposed by Guiggiani and Gigante [11], Guiggiani et al. [12] is used herein.

4 Loading velocity rates effects at FPZ

Rush [5] observed a direct relationship between loading rate, initial stiffness, peak stress value and peak load in quasi-brittle materials. Then, Wittman et al. [3] evaluated the effect of the loading rate on the value of G_f and the parameters of the bilinear cohesive law. The results show that at high loading rates the value of G_f decreases to a minimum value, whereas the critical crack opening, w_c, decreases. Therefore, to account the effects presented in Wittman et al. [3], the following equation provides an additional modification in the cohesive crack model to take into account the increase in loading rates. The modification refers to the correction of fracture energy as a function of the crack opening rate, $\dot{w}$[6]

The modification proposed by [6] has been defined as follows:

$$\sigma(\dot{w}, w) = \Xi(\dot{w}, w) = \Psi(\dot{w})f(w, G(\dot{w})) \tag{11}$$

where $f(w, G(\dot{w}))$ refers to the cohesive law modified by the fracture energy dependent on the loading rate, $G(\dot{w})$. $\Psi(\dot{w})$ is the viscous function. The dot over the variable indicates time variation. The $\Psi(\dot{w})$ is described as follows [15]:

$$\Psi(\dot{w}) = 1 + \left(\frac{\dot{w}}{\dot{w}_0}\right)^n \tag{12}$$

where $\dot{w}_0$ indicates a normalisation parameter for w and n is the exponent of rate dependence.

Additionally, $G(\dot{w})$ has been defined as follows [6]:

$$G(\dot{w}) = 1 - \left(\frac{\dot{w}}{\dot{w}_w}\right)^{n_w} \qquad for \quad \dot{w} \leq \dot{w}_w 0 \quad to \quad \dot{w} > \dot{w}_w \tag{13}$$

where $\dot{w}_w$ is the crack opening displacement rate and n_w is a parameter that governs the concrete behaviour[6].

5 The updated cohesive laws

The classic cohesive laws[16] $f(w, G(\dot{w}))$, will be updated to account the viscous effects,

$$\sigma = E\varepsilon \qquad for \quad \varepsilon \leq \varepsilon_c \tag{14}$$

$$\sigma_t(w) = f_t\left(1 - \frac{w}{w_c^{up}}\right) \qquad for \quad 0 \leq w \leq w_c^{up} \tag{15}$$

$$\sigma = 0 \qquad for \quad w > w_c \tag{16}$$

where ε_c refers to the limit in the elastic phase, σ_t^c represents the tensile strength of the material and w_c^{up} indicates the updated value for the critical crack opening, w_c, which is $w_c^{up} = G(\dot{w})w_c$:

The new bilinear cohesive law is following defined [6]:

$$\sigma = E\varepsilon \qquad for \quad \varepsilon \leq \varepsilon_c \tag{17}$$

$$\sigma_t(w) = f_t\left(1 - \frac{\left(f_t - f_t^{''}\right)}{w^{''}}\right)\frac{w}{G(\dot{w})} \qquad for \quad 0 \leq w \leq w_{up}^{''} \tag{18}$$

$$\sigma_t(w) = \frac{f_t^{''}}{w^{''} - w_c}\frac{w}{G(\dot{w})} + f''_t\left(1 - \frac{w^{''}}{w^{''} - w_c}\right) \qquad for \quad w_{up}^{''} \leq w \leq w_c^{up} \tag{19}$$

$$\sigma_t(w) = 0 \qquad for \quad w > w_c^{up} \tag{20}$$

where the variables $f_t^{''}$, $w^{''}$, $w_{up}^{''}$, w_c and w_c^{up} are defined as:

$$f_t^{''} = \frac{f_t^c}{3} \qquad w^{''} = \frac{0,8\ G_f}{f_t} \qquad w_{up}^{''} = w^{''}G(\dot{w}) \tag{21}$$

$$w_c = \frac{3,6\ G_f}{f_t}G(\dot{w}) \qquad w_c^{up} = w_c G(\dot{w}) \tag{22}$$

The exponential cohesive law updated by viscous effects is finally defined:

$$\sigma_t^{''} = E\varepsilon \qquad for \qquad \varepsilon \leq \varepsilon_c \tag{23}$$

$$\sigma_t(w) = f_t e^{\left(-\frac{f_t}{G_f}\frac{w}{G(\dot{w})}\right)} \qquad for \qquad w > 0 \tag{24}$$

Figure 1. Solid under tensile loading (a) Geometric and material properties (b) Mesh discretisation [9]

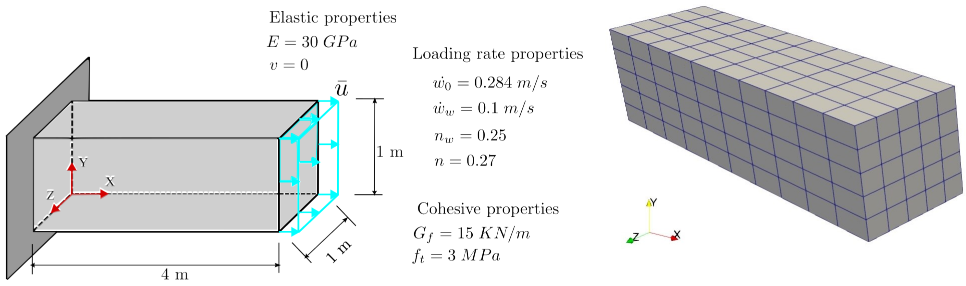

6 Applications

6.1 Application: Parallelepiped solid specimen on simple tensile test

The application defined in this work deals with a solid under tensile loading. The viscous-cohesive formulation is applied in a mode I fracture propagation. Figure 1 presents the geometric and material properties, whereas Figure 1 the mesh. The boundary mesh consists of 40 collocation points and 230 quadrilateral isoparametric linear boundary elements. The tensile loading is applied in 200 load steps. Analytical results can be found in literature[7–10]. This application can be found with more details in Almeida and Leonel [9]

Three loading rates were considere in this analyses, $10^{-7}\ m/s$, $10^{-5}\ m/s$ and $10^{-3}\ m/s$. Figure 2 presents force versus displacement curves for the three cohesive laws. As expected, increasing the rate leads to an apparent increasing in tensile strength of the material. Opposite behaviour was observed for the apparent fracturing energy. Thus, the increase in the intensity of external loads triggers the fracture process when high loading rates are applied. Furthermore, the critical crack opening reduces with increasing loading rates. This is an important feature of this approach, which represents the physical phenomenon observed experimentally [2, 5, 6]. So, the material tends to brittle behavior as the loading rate increases.

Figure 2. Force versus displacement curves considering viscous effects[9]

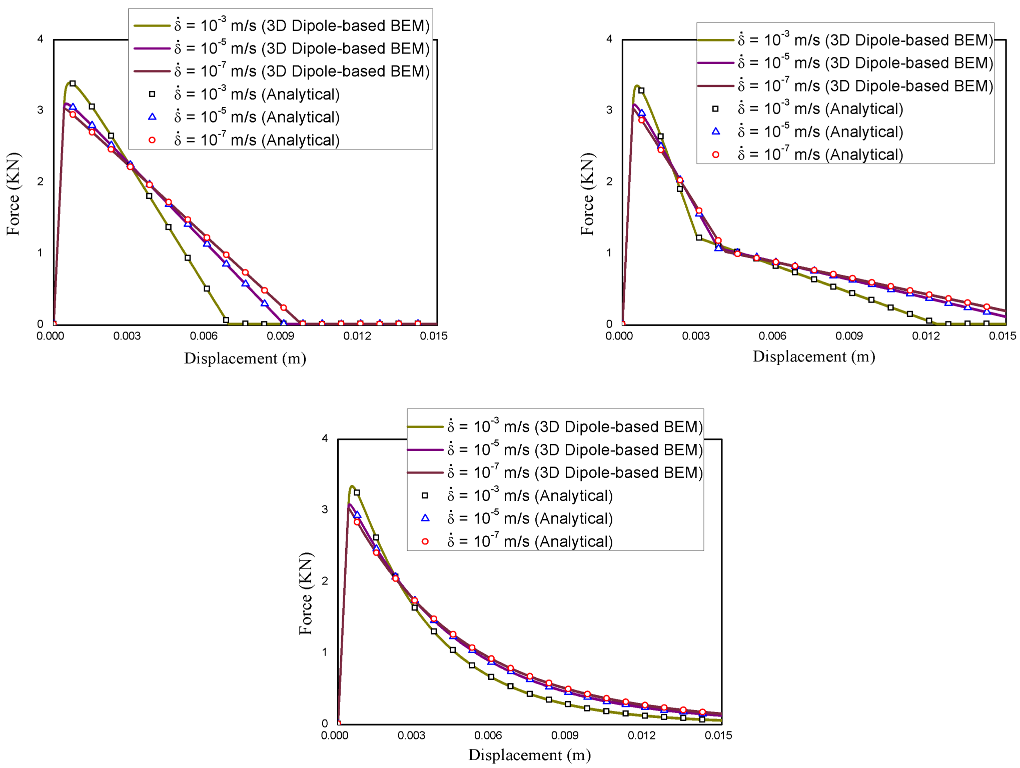

Figure 3 illustrates the displacement results provided by the viscous-cohesive dipole-based formulation along X direction in the final load step (200th load step). The figure shows the structural collapse due to separation of the solid in two independent parts.

Figure 3. Crack path and displacement (m) at 200th load step

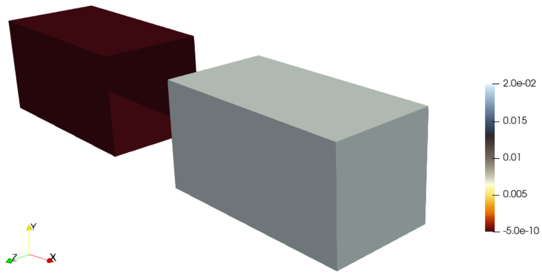

7 Conclusions

In this work, a tridimensional viscous-cohesive BEM formulation was proposed. Such formulation is based on dipoles of stresses, leading to an alternative approach to other classic BEM approaches. The propose formulation proved to be a powerful technique to the modelling of viscous-cohesive crack growth, and its robustness and efficiency can be demonstrated in the light of the example presented this work, considering analytical results from the literature. Future works include: Isogeometric analysis, enriched context and dynamic problems.

Acknowledgements. The authors are grateful to the Coordination for the Improvement of Higher Education Personnel – CAPES, for the scholarship provided to the first author

Authorship statement. The authors hereby confirm that they are the sole liable persons responsible for the authorship of this work, and that all material that has been herein included as part of the present paper is either the property (and authorship) of the authors, or has the permission of the owners to be included here.

References

[1] H. Oliveira and E. Leonel. Cohesive crack growth modelling based on an alternative nonlinear bem formulation. *Engineering Fracture Mechanics*, vol. 111, pp. 86–97, 2013.
[2] G. Ruiz, X. Zhang, R. Yu, P. Porras, E. Poveda, and del J. Viso. Effect of loading rate on fracture energy of high strength concrete. *Strain*, vol. 47, pp. 518–524, 2010.
[3] F. Wittman, P. Roelfstra, H. Mihashi, Y. Huang, X. Zhang, and N. Nomura. Influence of age of loading, water-cement ratio and rate of loading on fracture energy of concrete. *Materials and Structures*, vol. 20, pp. 103–110, 1987.
[4] Z. Bazant and R. Gettu. Rate effects and load relaxation in static fracture of concrete. *Aci Materials Journal*, vol. 89, pp. 456–468, 1992.
[5] H. Rush. Researches toward a general flexural theory for structural concrete. *Journal of the American Concrete Institute*, vol. 57, 1960.
[6] F. Santos and J. Sousa. A viscous-cohesive model for concrete fracture in quasi-static loading rate. *Engineering Fracture Mechanics*, vol. 228, pp. 106893, 2020.
[7] L. P. R. Almeida, E. T. Lima Junir, and J. C. C. Barbirato. Cohesive crack propagation analysis using a dipole BEM formulation with tangent operator. *Theoretical and Applied Fracture Mechanics*, vol. 109, pp. 102765, 2020a.
[8] L. P. R. Almeida, E. T. Lima Junir, and J. C. C. Barbirato. Probabilistic dipole BEM model for cohesive crack propagation analysis. *J Braz. Soc. Mech. Sci. Eng.*, vol. 44, pp. 485, 2022.
[9] L. P. R. Almeida and E. D. Leonel. The fracture failure modelling of three-dimensional structures composed of quasi-brittle materials subjected to different loading velocities rates by the dipole-based bem approach. *International Journal of Solids and Structures*, vol. 286-287, pp. 112595, 2024.
[10] L. P. R. Almeida and E. D. Leonel. Dipole-based bem formulation for three-dimensional cohesive crack propagation modelling. *International Journal for Numerical Methods in Engineering*, pp. e7535, 2024.
[11] M. Guiggiani and A. Gigante. A general algorithm for multidimensional cauchy principal value integrals in the boundary element method. *Journal of Applied Mechanics*, vol. 57, pp. 906–, 1990.

[12] M. Guiggiani, G. Krishnasamy, T. Rudolphi, and F. Rizzo. A general algorithm for the numerical solution of hypersingular boundary integral equations. *Journal of Applied Mechanics*, vol. 59, pp. 604–, 1992.
[13] C. Brebbia. *The Boundary Element Method for Engineers*. Pentech Press, London, 1978.
[14] L. P. R. Almeida, E. T. Lima Junir, and J. C. C. Barbirato. BEM-FORM model for the probabilistic response of circular tunnels in elastic media. *KSCE J Civ Eng*, vol. 24, pp. 2244–55, 2020b.
[15] A. Rosa, R. Yu, G. Ruiz, L. Saucedo, and J. Sousa. A loading rate dependent cohesive model for concrete fracture. *Engineering Fracture Mechanics*, vol. 82, pp. 195–208, 2012.
[16] A. Hillerborg, M. Modeer, and P. Peterson. Analysis of crack formation and crack growth in concrete by mean of failure mechanics and finite elements. *Cement and Concrete Research*, vol. 6, pp. 773–782, 1976.